



# Role of Limestone Addition in Improving the Initial Compressive Strength of Geopolymer Concrete for Corrosive Environment Repair



Arwinda Aribah Cahyani<sup>a</sup>, Nur Ahmad Husin<sup>a</sup>, Ridho Bayuaji<sup>a</sup>, Yuyun Tajunnisa<sup>a\*</sup>

<sup>a</sup>Department of Civil Infrastructure Engineering, Sepuluh Nopember Institute of Technology, Menur St. 127, Surabaya, 60116, Indonesia

## Abstract

Geopolymer Concrete (GC) is highly durable in corrosive environments, making it a viable material for repair. However, its initial compressive strength was below the 7 MPa required at 1-day age. Adding fine limestone (45  $\mu\text{m}$ ) can improve GC's density and early strength. This study explores the effects of adding 0, 3, 5, and 7% limestone and 1% sucrose superplasticizer to GC 16M. The compressive strength was tested at 1, 3, 7, and 28 days, along with slump, permeability, and resistivity tests to assess the durability. The results show that adding 5% limestone yields the optimal GC performance for repairing corrosive environments. The compressive strengths were 15.96, 28, 43, and 67.14 MPa at 3 days, 43 MPa at 7 days, and 67.14 MPa at 28 days, with a slump of 120 mm. The permeability and resistivity results were 0.128 E-16  $\text{m}^2$  and 57.87  $\text{k}\Omega\text{-cm}$ , indicating normal corrosion levels. These findings confirm that GC with 5% limestone meets the durability and strength requirements of repair materials in corrosive environments.

**Keywords:** Concrete repair material; Corrosive environment; Geopolymer concrete; Limestone

## 1. Introduction

One of the most significant challenges in modern construction is ensuring material durability under extreme and corrosive environmental conditions. Concrete structures often experience substantial degradation when exposed to corrosive environments, such as coastal areas or industrial zones with high corrosion levels. Corrosive environments can damage reinforcement by causing rust, which expands the reinforcement volume, thereby inducing cracks and spalling in the concrete [1]. Additionally, increased loads and changes in building use can lead to structural damage, impacting performance [2]. Reinforcement and repair of structures are necessary when cracks are detected to prevent collapse [3]–[6]. Therefore, developing repair materials that are more resistant to corrosive environments is a crucial priority to enhance structures' service life and reliability.

Geopolymer Concrete (GC) demonstrates exceptional durability when utilized in corrosive settings. Moreover, geopolymer concrete is produced using 100% waste materials, making it more environmentally friendly compared to Portland cement. The use of geopolymer concrete can reduce waste and carbon emissions that are harmful to the environment. Research conducted by Prusty et al. [7] on a geopolymer concrete mix consisting of 55% Class F Fly Ash (FA) and 45% Ground Granulated Blast Furnace Slag (GGBS) revealed substantial corrosion resistance, as evidenced by its microstructure analysis. Additionally, a study by Husin et al. [8] that employed Class C FA as a pozzolan recorded a compressive strength of 51.9 MPa, with the material's corrosion rate classified as low to moderate, as indicated by a resistivity test value of 14.42  $\text{k}\Omega\text{cm}$ . Geopolymer concrete is primarily formulated from pozzolans and alkaline activators, with fly ash (FA) being a prevalent pozzolan due to its high silicon and aluminum content. This composition facilitates a polymerization reaction that fosters robust bonding within the concrete [9], [10]. Collectively, these studies underscore the potential of geopolymer concrete as a viable repair material for environments prone to corrosion. Its primary benefits include reduced carbon emissions and enhanced resistance to chemical degradation compared to traditional Portland cement-based concrete [11]–[14]. Nevertheless, a significant challenge lies in its low early compressive strength, which is critical for applications in structural repairs.

The addition of limestone to geopolymer concrete mixtures has been identified as a potential solution to improve early compressive strength [15]. Studies such as [16] indicate that limestone not only acts as a filler that can fill microvoids in the concrete structure but also participates in the polymerization reaction, enhancing the material's density and strength. Moreover, limestone is relatively inexpensive and readily available, which can reduce the production costs of geopolymer concrete.

This study aims to evaluate the impact of limestone addition on the early compressive strength of geopolymer concrete, to develop it as Geopolymer Concrete for Repair (GCR) in corrosive environments. The primary focus is to identify the optimal proportion of limestone that can enhance early compressive strength without compromising corrosion resistance. The methodology includes early compressive strength testing at various limestone proportions and performance analysis of geopolymer concrete in corrosive environments.

The results of this study are expected to significantly contribute to the development of superior geopolymer concrete materials for structural repair applications in corrosive environments. Consequently, this research will provide more efficient and durable material solutions for the construction industry, particularly in the repair and maintenance of structures in corrosive environments.

## 2. Method

### 2.1. Materials

This research employs fly ash (FA) procured from the Nusantara Power Plant in Probolinggo, Indonesia, as a precursor. Based on X-ray fluorescence (XRF) analysis, the FA is classified as Class C, containing approximately 18% CaO, aligning with ASTM C618 standards [17]. The results of the XRF analysis are detailed in Table 4. X-ray diffraction (XRD) data, outlined in Table 1, reveal that the FA consists of 61.31% amorphous phase and 38.69% crystalline phase. This composition suggests a high reactivity of the FA, characterized by a substantial amorphous content. Such a high level of amorphous material is beneficial for the reaction of silicon and aluminum ions, which promotes the polymerization reactions necessary for geopolymer formation [18].

The fine aggregate (sand) used in this study is sourced from Lumajang. The material characterization of the sand is shown in Table 5. The sand's fineness modulus is 2.219, with particle gradation falling into zone 1 of coarse sand (Figure 1). The coarse aggregate (gravel) is obtained from a stone-crushing industry in Grati Pasuruan. The test results for the gravel material are presented in Table 5, with the particle gradation for gravel ranging from 10-20 mm shown in Figure 2.

Table 1. Crystalline Phase of Fly Ash (FA) (wt %)

Crystalline phase	Chemical formulas	Value (%)
Quartz	SiO <sub>2</sub>	5.06
Brownmillerite (Si,Mg)	Ca <sub>2</sub> Fe <sub>1.2</sub> Mg <sub>0.4</sub> Si <sub>0.4</sub> O <sub>5</sub>	7.78
Periclase	MgO	5.43
Magnetite	Fe <sub>3</sub> O <sub>4</sub>	2.94
Maghemite	Fe <sub>2</sub> O <sub>3</sub>	2.26
Anhydrite	CaSO <sub>4</sub>	2.33
Lime	CaO	0.51
Calcite magnesian	Ca <sub>0.9</sub> Mg <sub>0.1</sub> CO <sub>3</sub>	2.84
Iron alpha	Fe	0.26
Hematite	Fe <sub>2</sub> O <sub>3</sub>	1.13
C3A cubic	Ca <sub>3</sub> Al <sub>2</sub> O <sub>6</sub>	4.82
Mullite 3:2	(Al <sub>2</sub> O <sub>3</sub> ) <sub>3</sub> (SiO <sub>2</sub> ) <sub>2</sub>	2.09
Mullite 2:1	(Al <sub>2</sub> O <sub>3</sub> ) <sub>2</sub> (SiO <sub>2</sub> )	0.71
Rutile	TiO <sub>2</sub>	0.54
Andesine An50	(Rb <sub>0.811</sub> Al <sub>0.062</sub> )(Al <sub>10.997</sub> Si <sub>3.003</sub> O <sub>8</sub> )	-
Hkl_phase		61.31

Table 2. Spesification of Sodium Metasilicate Pentahydrate (Granular)  $\text{Na}_2\text{SiO}_3 \cdot 5\text{H}_2\text{O}$

Parameter	Test Standart (HG/T2568-08)	Test Result
Sodium oxide ( $\text{Na}_2\text{O}$ ) %	28.70-30.00	29.00
Silica ( $\text{SiO}_2$ ) %	27.80-29.20	29.11
Water Insoluble (%)	$\leq 0.05$	0.02
Fe (ppm)	$\leq 100$ ppm	54
Whitness (%)	$\geq 80$	92
Bulk Density	0.8-0.97 g/cc	0.95
PH of 1.0% Solution	12-13	12.50
Melting Point	72.2° C	72.2° C
Particular Size % (16-30 mesh)	$\geq 90$	95

Table 3. Spesification of Sodium Hydroxide (flake) NaOH

Items	Test Result
NaOH	98.88 %
$\text{Na}_2\text{CO}_3$	0.42 %
NaCl	0.01 %
$\text{Fe}_2\text{O}_3$	0.001 %

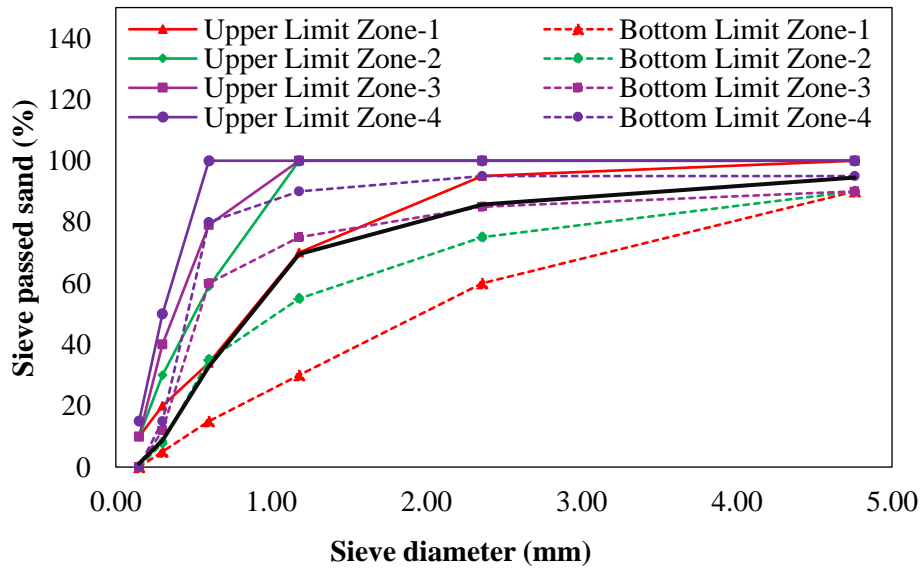


Figure 1. Fines Aggregate Sieve Analysis

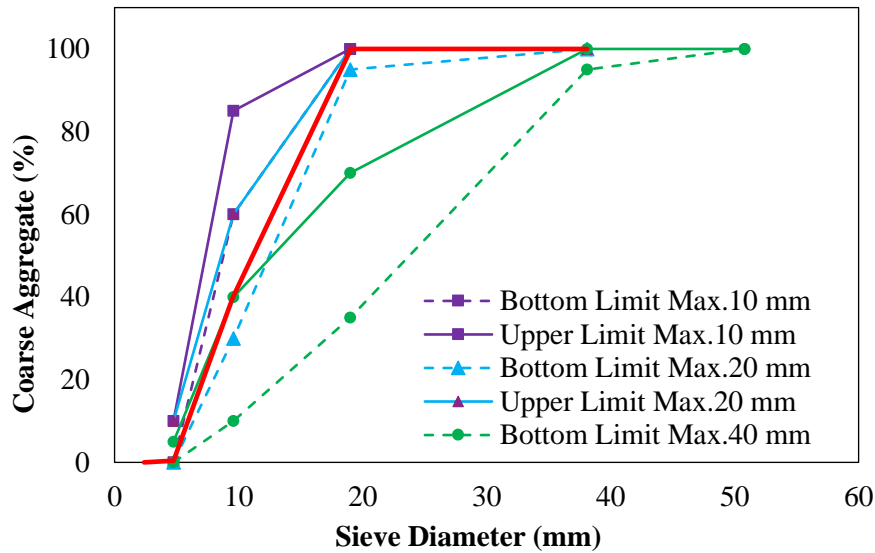


Figure 2. Coarse Aggregate Sieve Analysis

The alkali activator used includes solid sodium metasilicate pentahydrate ( $\text{Na}_2\text{SiO}_3 \cdot 5\text{H}_2\text{O}$ ) in granular form and sodium hydroxide ( $\text{NaOH}$ ) in flake form. The specifications for  $\text{Na}_2\text{SiO}_3 \cdot 5\text{H}_2\text{O}$  are presented in Table 2 while the specifications for  $\text{NaOH}$  are detailed in Table 3.

Sucrose is utilized as a superplasticizer (SP) in this study to enhance the workability of geopolymer concrete. Additionally, limestone is used as an additive to improve the early-age hydration process of the concrete and enhance its density due to its fine particle size [15], [19]–[21]. The limestone used in this research has a particle size above 45  $\mu\text{m}$ , with 83.56% retained, as determined by the Particle Size Distribution (PSD) test.

Table 4. Oxide Composition Fly Ash (wt %)

Materials	$\text{SiO}_2$	$\text{Al}_2\text{O}_3$	$\text{Fe}_2\text{O}_3$	$\text{CaO}$	$\text{MgO}$	$\text{SO}_3$	Na	K	Other
FA	37,06	14,78	13,96	17,91	9,22	1,73	1,41	0.89	3.04

Table 5. Aggregate Properties

Aggregate	Grain size (mm)	Density	Moisture content (%)	Absorption (%)	Weight Volume (gr)	Abration (%)	Modulus
Coarse	10-20	2.73	0.47	1.16	1326.67	17.72	3.59
Fines	< 5 mm	2.81	2.63	0.194	1604.44	-	

Table 6. Mix Design for GCR ( $\text{kg}/\text{m}^3$ )

Sample code	FA	Sand	Gravel	Alkali activator		SP	Limestone ( $\text{CaCO}_3$ )	Water
				$\text{NaOH}$	$\text{Na}_2\text{SiO}_3 \cdot 5\text{H}_2\text{O}$			
LM0-S1	595.884	526.751	1192.623	53.500	55.451	5.959	0	129.40
LM3-S1	595.884	526.751	1192.623	53.500	55.451	5.959	17.876	129.40
LM5-S1	595.884	526.751	1192.623	53.500	55.451	5.959	29.794	129.40
LM7-S1	595.884	526.751	1192.623	53.500	55.451	5.959	41.712	129.40
LM0-S2	595.884	526.751	1192.623	53.500	55.451	11.918	0	129.40
LM3-S2	595.884	526.751	1192.623	53.500	55.451	11.918	17.876	129.40
LM5-S2	595.884	526.751	1192.623	53.500	55.451	11.918	29.794	129.40
LM7-S2	595.884	526.751	1192.623	53.500	55.451	11.918	41.712	129.40

### 2.2. Mix Proportion

The composition of the geopolymer binder (GCR) investigated in this study is shown in Table 6. This research employs a NaOH molarity of 16 M for all GCR variations produced. A 16 Molar concentration was chosen due to its high compressive strength, equivalent to 65 MPa at 28 days of age, according to previous research. The molar ratio of NaOH to  $\text{Na}_2\text{SiO}_3 \cdot 5\text{H}_2\text{O}$  is 1:1. The variations used to determine the optimal GCR composition include different levels of superplasticizer (SP) and limestone. The SP (sucrose) content variations are set at 1% and 2% of the required fly ash, based on previous studies [8]. The limestone content variations used are 0%, 3%, 5%, and 7% of the required fly ash, according to studies by [16], [22], [23].

### 2.3. Mixing and Curing

The geopolymer binder (GCR) was mixed using a dry mixing method. The mixing process began with the preparation of geopolymer cement by grinding fly ash and alkali activator using 25 iron balls in a ball mill at a speed of 500 rpm (Figure 4). Once the cement was finely ground and removed from the ball mill, it was weighed to determine the percentage of cement loss during the grinding process. The percentage of ground cement was then used to calculate the required amounts of aggregates and other materials.

The concrete production process started by adding gravel and sand, which were mixed for 2 minutes. Sucrose SP was then added and mixed for another 2 minutes. Subsequently, the geopolymer cement was added and mixed for 5 minutes. Limestone was incorporated into the mixture after the geopolymer cement and mixed for 2 minutes. Once the dry mixture was homogeneous, water was added gradually. The wet mixture was then mixed for 7 minutes to allow the components to react completely, forming fresh GCR concrete.

The curing method employed for the samples was ambient curing at the temperature of  $30 \pm 2^\circ\text{C}$ . The samples were demolded one day after casting, placed in plastic bags, and stored in a container box at room temperature. The mixing and curing processes can be seen in Figure 3.

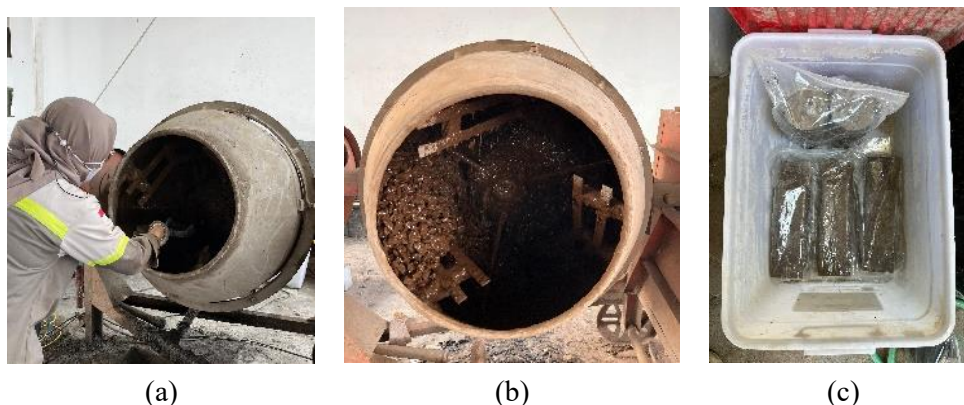


Figure 3. Mixing and Curing, (a) Mixing Procedure, (b) Concrete Mixer, (c) Ambient Curing



Figure 4. Dry Mixing Method Equipment, (a) Ball Mill Machine, (b) Iron Balls

2.4. Testing for Early Strength Concrete

The testing conducted to meet the standards for repair materials follows ASTM C1107 [24]. The compressive strength testing procedure adheres to ASTM C39, requiring the early compressive strength to meet the values specified in Table 7. The minimum slump value achieved should be between 60-180 mm with a maximum aggregate size of 20 mm. The resistivity testing, conducted according to ASTM B193, determines the geopolymer concrete's resistance to corrosion. Permeability testing follows ASTM C642 procedures to assess the concrete's ability to resist the penetration of water, air, and other liquids through its pores.

Table 7. Initial Compressive Strength Requirements for Repair Materials Standart [24]

Testing	1 day	3 days	7 days	28 days
Compressive Strength (MPa)	7.0	17.0	24.0	34.0

3. Results and Discussion

3.1. Slump Test

The slump testing procedure followed ASTM C143-2015 to determine the workability of the GCR. The slump test results are presented in Table 8.

Table 8. Compressive Strength and Slump

Sample Code	Compressive Strength (MPa)				Slump Test (mm)
	1 day	3 days	7 days	28 days	
LM0-S1	4.24	20.12	36.92	46.98	150
LM3-S1	8.79	27.88	34.55	53.90	120
LM5-S1	15.96	28.10	43.46	67.14	120
LM7-S1	18.38	34.46	44.99	66.89	120
LM0-S2	4.24	20.29	37.90	49.61	160
LM3-S2	2.16	21.31	39.00	49.06	200
LM5-S2	5.60	26.65	46.90	46.52	210
LM7-S2	4.92	21.69	24.45	33.74	215

Based on Table 8, all variations met the minimum slump value of 60 mm, ensuring the workability of the concrete. The slump value also increased as the superplasticizer content increased from 1% to 2%. Additionally, increasing the limestone content from 0% to 3%, 5%, and 7% also results in a higher slump value for the GCR. This is due to the microparticle size of limestone, which enhances the flowability of concrete [25]. The slump test results are shown in Figure 5.



Figure 5. Slump Test Results

### 3.2. Compressive Strength

Compressive strength tests were conducted at 1, 3, 7, and 28 days, adhering to the ASTM C1107 standards for minimum repair material requirements. The tests were performed using a Universal Testing Machine (UTM) with a 200-ton capacity (Figure 7). The results indicate that compressive strength increases with higher limestone content when using 1% superplasticizer. Conversely, variations with 2% superplasticizer tend to show a decrease in compressive strength as the limestone content increases. An increase in the superplasticizer content from 1% to 2% reduces the compressive strength by up to 65%. Variations LM3-S1, LM5-S1, and LM7-S1 variants meet the minimum early-age compressive strength standards for repair materials (Figure 6).

For chloride environments, concrete must achieve a minimum compressive strength of 35 MPa. Figure 6 shows that all GCR variations meet the minimum requirement for concrete in chloride environments at 28 days. The best compressive strength was observed for LM5-S1, reaching 67.14 MPa at 28 days. Figure 6 shows that the LM5-S1 variation meets the minimum repair material standards according to ASTM C1107 and can be developed for structural repair in corrosive environments.

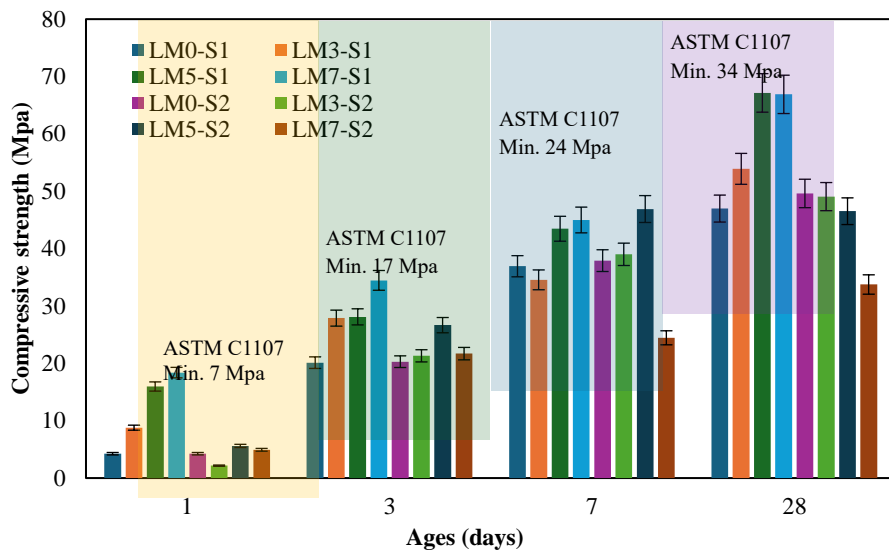


Figure 6. Compressive Strength Test Results



Figure 7. Universal Testing Machine

### 3.3. Resistivity

Resistivity testing was conducted to determine the concrete's ability to resist electric current. Concrete with high electrical resistivity is resistant to corrosion. The LM5-S1 variation was assessed at 56 days of age. The resistivity test was conducted using Resipod Proceq. The resistivity values are compared against the standard thresholds for corrosion levels, as outlined in Table 9.

Table 9. Relationship Between Resistivity and Corrosion Levels

Resistivity (k-Ωcm)	Corrosion rate
$\rho \geq 12$	No corrosion occurred
$8 < \rho < 12$	possibility of corrosion occurred
$\rho < 8$	corrosive

Sources: Operating Instruction Resistivity Tester PROCEQ

The resistivity test results for the LM5-S1 samples at 56 days are presented in Table 10. The average resistivity for specimens at the ages of 7 is 21.28 kΩcm, while specimens aged 28 years had average resistivities of 58.56 kΩcm, respectively. Table 10 shows result of the increasing resistivity trend of the geopolymer concrete as it aged from 7 days to 56 days. The resistivity test setup is shown in Figure 8.

Table 10. Resistivity Test Results of Geopolymer Concrete Coated with 5% Limestone and 1% Sucrose

Variation	Ages (days)	Sample	Resistivity			Averages	Deviation	Classification
LM5-S1	7	1	24.40	21.90	20.10	21.28	21.28	No corrosion occurred
			22.40	21.80	21.60			
		2	20.90	22.70	19.40			
			21.50	19.60	20.00			
		3	21.30	21.50	18.50			
			19.10	24.20	22.10			
	56	1	51.30	64.80	57.50	58.56	58.56	No corrosion occurred
			52.40	55.70	62.80			
			62.70	69.80	55.30			
			60.40	60.50	58.70			
2	54.30	59.70	52.20					
	57.60	58.30	60.10					



Figure 8. Resistivity Test Setup

### 3.4. Permeability

The permeability testing determines the concrete’s ability to absorb and transmit water and other liquids. This test is crucial because the permeability of concrete is closely related to its durability or resistance to various types of damage, including reinforcement corrosion, freezing and thawing, and chemical attacks. Lower permeability values indicate better concrete performance in corrosive environments. The quality classification of the concrete was based on the guidelines provided in the Operating Instruction Manual for the TORRENT permeability tester (Table 11).

Based on the permeability test results shown in Table 12, the LM5-S1 variation had an average permeability value of  $0.128 \times 10^{-16} \text{ m}^2$  with a standard deviation of 0.034. This average value falls within the "Normal" classification



according to the concrete quality classification table (Table 11). Specimen 1 had a permeability value of  $0.08 \times 10^{-16}$  m<sup>2</sup>, which falls into the "Good" classification. This indicates that Specimen 1 performs exceptionally well at preventing the absorption of water and other liquids, thus exhibiting high durability in corrosive environments. Specimens 2 and 3 had permeability values of  $0.15 \times 10^{-16}$  m<sup>2</sup> and  $0.155 \times 10^{-16}$  m<sup>2</sup>, respectively, both classified as "Normal". These results suggest that these two specimens have reasonably good ability to resist water and other liquid absorption, although not as effectively as Specimen 1.

Table 11. Classification of Concrete Quality Based on the Tested Permeability

Concrete quality	Index	kT [10 <sup>-16</sup> m <sup>2</sup> ]
Atrocious	5	>10
Bad	4	1.0-10
Normal	3	0.1-1.0
Good	2	0.01-0.1
Excellent	1	<0.01

Sources: Operating Instruction Permeability Tester TORRENT

Table 12. Permeability Test Results of Geopolymer Concrete with 5% Limestone and 1% Sucrose

Variation	Specimen Number	Permeability		Averages	Standard Deviation	Classification
		kT	L	kT		
		(E-16 m <sup>2</sup> )	(mm)	(E-16 m <sup>2</sup> )		
LM5-S1	1	0.08	18.9	0.128	0.034	Normal
	2	0.15	26.5			
	3	0.155	26.4			

Overall, the LM5-S1 variation demonstrated good performance in terms of permeability, with most permeability values falling within the "Normal" classification and one specimen classified as "Good". These results indicate that the LM5-S1 variant has good potential for use in corrosive environments. The GCR permeability testing setup is shown in Figure 9.

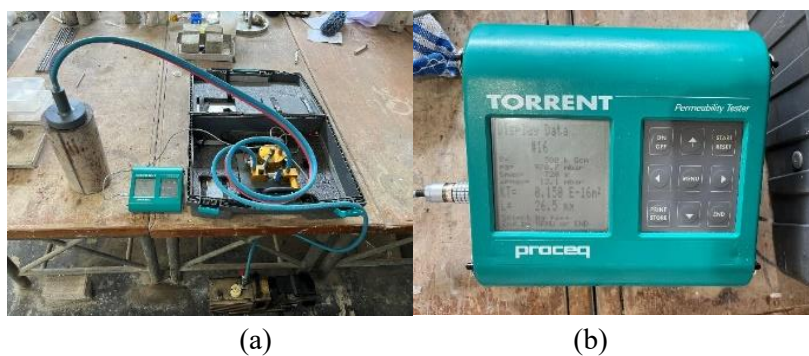


Figure 9. Permeability Test Machine, (a) Permeability Setup, (b) Torrent Permeability Tester

#### 4. Conclusions

Various tests were conducted to determine the optimal composition for the repair of geopolymer concrete, revealing several key findings. The LM5-S1 variant demonstrated good performance, meeting the minimum compressive strength standards for concrete repair. Resistivity and permeability tests indicated that the LM5-S1 variant performs well when GCR is applied in corrosive environments, making it a candidate for future research on developing repair materials for such conditions. Additionally, geopolymer concrete with the addition of limestone shows significant potential as a repair material in corrosive environments due to its enhanced resistance to chemical attack and high

durability. For future research, it is recommended to conduct bond strength testing on repair materials to determine the bond strength between geopolymer concrete and existing concrete.

### Acknowledgment

This research was funded by the Ministry of Research and Culture of Indonesia, through the BIMA Kemendikbud program, 2024. We express our gratitude for their support and contribution which made this study possible.

### References

- [1] T. Kannangara, P. Joseph, S. Fragomeni, and M. Guerrieri, "Existing theories of concrete spalling and test methods relating to moisture migration patterns upon exposure to elevated temperatures – A review," *Case Stud. Constr. Mater.*, vol. 16, 2022.
- [2] S. C. Lin, Z. Q. Hu, J. Q. Han, B. Yang, and M. Elchalakani, "Failure time of reinforced concrete column under blast load," *Structures*, vol. 53, no. April, pp. 1122–1134, 2023.
- [3] H. Jin, Y. Wei, Y. Zhang, Z. Huang, and L. Liu, "Compressive performance of underwater concrete columns strengthened by nondispersive mortar and stainless steel tubes," *Case Stud. Constr. Mater.*, vol. 19, 2023.
- [4] R. V. Makawana, P. V. Patel, and D. D. Joshi, "Seismic performance of exterior RC beam-column junction strengthened with Stainless Steel Wire Mesh (SSWM)," *Mater. Today Proc.*, 2023.
- [5] Y. Blikharskyy, J. Selejdak, R. Vashkevych, N. Kopiika, and Z. Blikharskyy, "Strengthening RC eccentrically loaded columns by CFRP at different levels of initial load," *Eng. Struct.*, vol. 280, p. 115694, 2023.
- [6] A. G. Saad, M. A. Sakr, and T. M. El-korany, "The shear strength of existing non-seismic RC beam-column joints strengthened with CFRP Sheets: Numerical and analytical study," *Eng. Struct.*, vol. 291, p. 116497, 2023.
- [7] J. K. Prusty and B. Pradhan, "Influence of chloride ions on strength and microstructure of geopolymer concrete containing fly ash, and blend of fly ash-GGBS," *Mater. Today Proc.*, vol. 65, pp. 925–932, 2022.
- [8] N. A. Husin, R. Bayuaji, Y. Tajunnisa, M. S. Darmawan, and P. Suprobo, "Performance of high calcium fly ash based geopolymer concrete in chloride environment," *Int. J. GEOMATE*, vol. 19, no. 74, pp. 107–113, 2020.
- [9] A. Raza, B. Ahmed, M. H. El Ouni, and W. Chen, "Mechanical, durability and microstructural characterization of cost-effective polyethylene fiber-reinforced geopolymer concrete," *Constr. Build. Mater.*, vol. 432, p. 136661, 2024.
- [10] Y. Tajunnisa, M. Sugimoto, T. Uchinuno, T. Sato, Y. Toda, A. Hamasaki, T. Yoshinaga, K. Shida, and Mitsuhiro, "Effect of Ggbfs and micro-silica on mechanical properties, shrinkage and microstructure of alkali-activated fly ash mortar," *Int. J. GEOMATE*, vol. 13, no. 39, pp. 87–94, 2017.
- [11] M. Amran, A. A. Fakhri, S. H. Chu, R. Fediuk, S. Haruna, A. Azevedo, and N. Vatin, "Long-term durability properties of geopolymer concrete: An in-depth review," *Case Stud. Constr. Mater.*, vol. 15, p. e00661, 2021.
- [12] Y. S. Wang, K. Di Peng, Y. Alrefaei, and J. G. Dai, "The bond between geopolymer repair mortars and OPC concrete substrate: Strength and microscopic interactions," *Cem. Concr. Compos.*, vol. 119, p. 103991, 2021.
- [13] S. H. G. Mousavinejad and M. Sammak, "Strength and chloride ion penetration resistance of ultra-high-performance fiber reinforced geopolymer concrete," *Structures*, vol. 32, pp. 1420–1427, 2021.

- [14] P. Pradhan, S. Dwibedy, M. Pradhan, S. Panda, and S. K. Panigrahi, “Durability characteristics of geopolymer concrete - Progress and perspectives,” *J. Build. Eng.*, vol. 59, p. 105100, 2022.
- [15] J. Camiletti, A. M. Soliman, and M. L. Nehdi, “Effect of limestone addition on early-age properties of ultra high-performance concrete,” *Proc. Inst. Civ. Eng. Constr. Mater.*, vol. 167, no. 2, pp. 65–78, 2014.
- [16] D. Kubatova, I. Khongova, M. Krejci Kotlanova, A. Zezulova, and M. Bohac, “The use of limestone sludge for the geopolymer preparation,” *IOP Conf. Ser. Mater. Sci. Eng.*, vol. 1205, no. 1, p. 012002, 2021.
- [17] ASTM-C618-19, “Standard Specification for Coal Fly Ash and Raw or Calcined Natural Pozzolan for Use,” *Annu. B. ASTM Stand.*, pp. 3–6, 2019.
- [18] A. F. Jiménez and A. Palomo, “Composition and microstructure of alkali activated fly ash binder: Effect of the activator,” *Cem. Concr. Res.*, vol. 35, no. 10, pp. 1984–1992, 2005.
- [19] C. L. Chan and M. Zhang, “Effect of limestone on engineering properties of alkali-activated concrete: A review,” *Constr. Build. Mater.*, vol. 362, p. 129709, 2023.
- [20] C. Li and L. Jiang, “Utilization of limestone powder as an activator for early-age strength improvement of slag concrete,” *Constr. Build. Mater.*, vol. 253, p. 119257, 2020.
- [21] W. Huang, H. K. Kamyab, W. Sun, and K. Scrivener, “Effect of cement substitution by limestone on the hydration and microstructural development of ultra-high performance concrete (UHPC),” *Cem. Concr. Compos.*, vol. 77, pp. 86–101, 2017.
- [22] A. D. Baykar, A. N. Sangale, P. M. Kurhade, and P. P. D. Gunaware, “Geopolymer Concrete Using Lime , With Ambient Curing,” vol. 6, no. 3, pp. 176–182, 2019.
- [23] Y. Wu, P. Tang, H. Lv, W. Wei, S. Zhou, and K. Liu, “Degradation of the bond performance between composite limestone powder concrete and steel bars under a sulfate freeze–thaw environment,” *Constr. Build. Mater.*, vol. 369, p. 130515, 2023.
- [24] A. B. Hardness, V. Hardness, S. Hardness, K. Hardness, and S. Hardness, “Standard Specification for Packaged Dry, Hydraulic-Cement Grout (Nonshrink),” vol. 86, pp. 10–11, 2012.
- [25] J. Camiletti, A. M. Soliman, and M. L. Nehdi, “Effects of nano- and micro-limestone addition on early-age properties of ultra-high-performance concrete,” *Mater. Struct. Constr.*, vol. 46, no. 6, pp. 881–898, 2013.